

Thermoelectric properties of $\text{Ca}_3\text{Co}_4\text{O}_{9+\delta}$ with Lu substitution

G. D. Tang · Z. H. Wang · X. N. Xu · L. Qiu ·
L. Xing · Y. W. Du

Received: 31 October 2009 / Accepted: 1 April 2010 / Published online: 13 April 2010
© Springer Science+Business Media, LLC 2010

Abstract A series of $\text{Ca}_{3-x}\text{Lu}_x\text{Co}_4\text{O}_{9+\delta}$ ($x = 0, 0.1, 0.2$, and 0.4) has been prepared by sol–gel method. The effects of Lutetium substitution on thermoelectric properties of $\text{Ca}_3\text{Co}_4\text{O}_{9+\delta}$ have been systematically investigated from 4 to 335 K. With the partial substitution of Lu^{3+} for Ca^{2+} , the resistivity and thermopower for Lu-doped samples increase, while their thermal conductivity decreases. The dimensionless figure of merit for $\text{Ca}_{2.8}\text{Lu}_{0.2}\text{Co}_4\text{O}_{9+\delta}$ material ($ZT = 0.032$) is about five times better than that for $\text{Ca}_3\text{Co}_4\text{O}_{9+\delta}$ ($ZT = 0.007$) at 335 K. Strikingly, for Lu-doped samples, the thermopower exhibits a steeper upturn at low temperatures.

Introduction

Thermoelectric materials have attracted much interest as a clean energy-conversion system [1]. The high performance of thermoelectric materials is determined by the dimensionless thermoelectric figure of merit $ZT = S^2 T / \rho \kappa$, where T , S , κ , and ρ are the absolute temperature, the thermopower, the thermal conductivity, and the electrical resistivity, respectively. Thus, large thermopower (absolute value of thermopower), low electrical resistivity, and low thermal conductivity are required for optimum thermoelectric materials. Since Terasaki et al. [2] reported that

NaCo_2O_4 had a large thermopower and a high conductivity, the layer cobalt oxides have been studied extensively [2–6]. In this family, $\text{Ca}_3\text{Co}_4\text{O}_{9+\delta}$ system shows good thermoelectric performance and large thermopower [7–11]. The $\text{Ca}_3\text{Co}_4\text{O}_{9+\delta}$ system has been considered to be a good candidate of thermoelectric materials due to its thermal and chemical stability at high temperature in air. However, for practice use its thermoelectric performance must be further improved. So far, many experimental investigations have been carried out to enhance its thermoelectric properties [9–11]. One approach to improve the thermoelectric properties is doping Ca sites with metals such as rare earths (Dy, Gd, Eu, La, Nd, Y), alkali metals, or alkaline earth metals [10–17]. With partial rare earth substitution, its thermopower and thermoelectric performance increase, while its thermal conductivity decreases [13, 16, 17]. Lu element doping inspires our interest for believing that doping with heavy ions can enhance phonon scattering and further suppress the lattice contribution to the thermal conductivity. This will contribute to the improvement of thermoelectric efficiency for $\text{Ca}_3\text{Co}_4\text{O}_{9+\delta}$ system. In this study, we synthesize the polycrystalline $\text{Ca}_{3-x}\text{Lu}_x\text{Co}_4\text{O}_{9+\delta}$ samples and undertake systematical study on the effect of Lu doping on the thermoelectric properties.

Experimental

$\text{Ca}_{3-x}\text{Lu}_x\text{Co}_4\text{O}_{9+\delta}$ ($x = 0, 0.1, 0.2$, and 0.4) powders were prepared using sol–gel method. The reagent grade CaCO_3 , $\text{Co}(\text{NO}_3)_2 \cdot 6\text{H}_2\text{O}$, $\text{Lu}(\text{NO}_3)_3 \cdot 6\text{H}_2\text{O}$, and citric acid monohydrate in specific proportion were dissolved in distilled water. The citrate solution was dehydrated at 353 K. The resulted uniform was crushed and heated to 473 K for 2 h to remove the moisture of gel. The obtained carbonaceous

G. D. Tang · Z. H. Wang (✉) · X. N. Xu · L. Qiu · L. Xing ·
Y. W. Du
National Laboratory of Solid State Microstructures and Physics
Department, Nanjing University, 210093 Nanjing, China
e-mail: zhwang@nju.edu.cn

G. D. Tang · Y. W. Du
Jiangsu Provincial Laboratory for NanoTechnology, 210093
Nanjing, China

xerogel was then calcined at 823 K for 3 h in air. After being cooled to room temperature, the obtained powders were ground and sintered at 1173 K for 12 h, then pressed into pellets. These pellets were annealed at 1173 K for 36 h under O₂ atmosphere. Finally, black ceramic pellets were obtained.

X-ray diffraction (XRD) analysis was carried out using a Rigaku D/Max-gA diffractometer with Cu K α radiation. The actual composition is determined by inductively coupled plasma (ICP) method. All the thermoelectric properties (thermopower, thermal conductivity, and electrical resistivity) were measured using a physical property measurement system (PPMS) from 4 to 335 K.

Results and discussion

Figure 1 presents the XRD patterns for Ca_{3-x}Lu_xCo₄O_{9+δ} ($x = 0, 0.1, 0.2$, and 0.4) samples. All the diffraction peaks are identical to the standard JCPDS card (No. 21-0139) of Ca₃Co₄O_{9+δ}. In order to display the effect of Lu doping on Ca₃Co₄O_{9+δ} lattice, we show the enlarged (002) and (004) diffraction peaks in the left and right inset of Fig. 1, respectively. It can be seen that the diffraction peaks (002) and (004) shift from a low angle to a high angle with the increase in Lu content. The refined lattice parameters are given in Table 1. From Table 1, we can see that the lattice parameters a , b_1 , b_2 , and c decreases simultaneously with the increasing Lu content, which is consistent with the fact that Lu³⁺ ion has a smaller ionic radius when compared with that of Ca²⁺ ion in these samples. The actual composition is Ca/Co/Lu = 2.87:4:0.11 for Ca_{2.9}Lu_{0.1}Co₄O_{9+δ}, Ca/Co/Lu = 2.78:4:0.21 for Ca_{2.8}Lu_{0.2}Co₄O_{9+δ}, and Ca/Co/Lu = 2.58:4:0.42 for Ca_{2.6}Lu_{0.4}Co₄O_{9+δ}, which is very

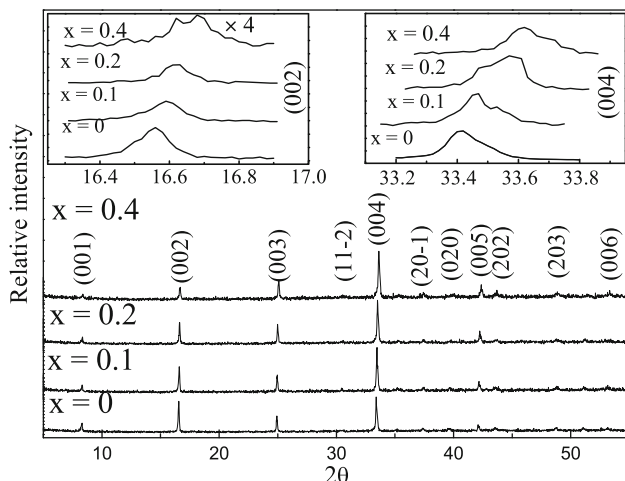


Fig. 1 XRD patterns for Ca_{3-x}Lu_xCo₄O_{9+δ} ($x = 0, 0.1, 0.2$, and 0.4). The left inset shows the enlarged (002) diffraction peak and the right inset shows the enlarged (004) peak

Table 1 Lattice parameters a , b_1 , b_2 , c , and β for Ca_{3-x}Lu_xCo₄O_{9+δ} ($x = 0, 0.1, 0.2$, and 0.4) samples. Here b_1 and b_2 are the b -axis length for [Ca₂Co₃] and [CoO₂] subsystems, respectively

x	a (nm)	b_1 (nm)	b_2 (nm)	c (nm)	β (°)
0	0.4837 (6)	0.4556 (5)	0.2818 (9)	1.0833 (1)	98.06 (2)
0.1	0.4825 (1)	0.4540 (3)	0.2808 (4)	1.0815 (1)	98.16 (1)
0.2	0.4817 (5)	0.4525 (7)	0.2800 (2)	1.0796 (4)	98.21 (1)
0.4	0.4814 (5)	0.4514 (6)	0.2781 (9)	1.0765 (5)	98.40 (3)

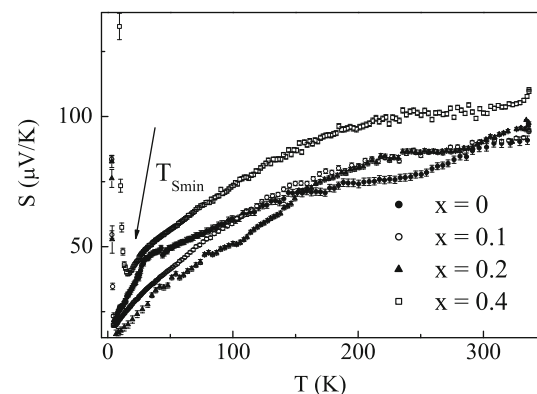


Fig. 2 Temperature dependence of thermopower in Ca_{3-x}Lu_xCo₄O_{9+δ} ($x = 0, 0.1, 0.2$, and 0.4) samples

close to the nominal composition. These results indicate that Lu³⁺ ions are really doped into Ca²⁺ sites.

Figure 2 shows the temperature dependence of thermopower (S) for Ca_{3-x}Lu_xCo₄O_{9+δ} ($x = 0, 0.1, 0.2$, and 0.4) from 4 to 335 K. The positive S indicates the hole conduction nature in Ca_{3-x}Lu_xCo₄O_{9+δ} ceramics. For all samples, S increases as the temperature increases from 16 K. Above 150 K, S is enhanced by Lu doping and reaches 110 μ V/K at 335 K for Ca_{2.6}Lu_{0.4}Co₄O_{9+δ} material. Between $T_{S\text{min}}$ and 100 K, the undoped Ca₃Co₄O_{9+δ} has a higher S than 0.1- and 0.2-doped samples with $x = 0.1$ and 0.2 . The reason needs to be studied further. When the temperature is lower than 16 K, the behavior of S for Lu-doped ceramics is different from that for Ca₃Co₄O_{9+δ}. A minimum S is observed at $T_{S\text{min}}$ which depends on the Lu doping level. On further cooling, S shows a steeper upturn.

As to the observed S upturn at low temperatures, a possible explanation is strong spin fluctuation effects [7], which was also observed in valence fluctuation systems and/or other cobalt oxides [18]. The susceptibility (χ) for Ca_{3-x}Lu_xCo₄O_{9+δ} ($x = 0, 0.1, 0.2$, and 0.4) samples is measured in the field-cooling mode under a magnetic field of 2 kOe. The temperature dependence of susceptibility ($\chi-T$) is shown in Fig. 3. It can be seen that χ slowly increases as the temperature decreases from 200 K, then

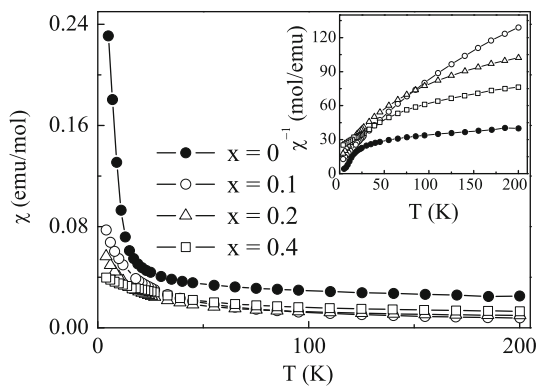


Fig. 3 Temperature dependence of susceptibility (χ) in $\text{Ca}_{3-x}\text{Lu}_x\text{Co}_4\text{O}_{9+\delta}$ ($x = 0, 0.1, 0.2$, and 0.4). The inset shows the temperature dependence of the inverse susceptibility for these samples

abruptly below 25 K. For all the doped samples, χ is suppressed by Lu doping in the whole studied temperature range. In the inset of Fig. 3, we plot the curves of inverse susceptibility ($1/\chi$). It is found that the magnetic behaviors of $\text{Ca}_{3-x}\text{Lu}_x\text{Co}_4\text{O}_{9+\delta}$ with $x = 0.1, 0.2$, and 0.4 above 100 K are paramagnetism and obey the Curie–Weiss law. The negative Weiss constant values suggest the presence of strong antiferromagnetic interaction at low temperatures. The samples with $x = 0.1, 0.2$, and 0.4 do not exhibit a clear ferrimagnetic transition which was observed in $\text{Ca}_3\text{Co}_4\text{O}_{9+\delta}$ [19]. Our results are consistent with previous reports that the ferrimagnetic transition is suppressed by M (M represents Sr, Y, Bi, Ti, Ce) doping into Ca sites for a $\text{Ca}_{3-x}\text{M}_x\text{Co}_4\text{O}_{9+\delta}$ system [10, 19, 20]. Because there is no magnetic ordering in these materials, weaker magnetic correlation between the Co ions results in the spin fluctuation. The spin fluctuation implies the weakly temperature-dependent susceptibility [21], consistent with the observed behavior of χ in Fig. 3.

According to Koshiba's report, the thermopower in misfit-layered cobaltite could be attributed to spin entropy of the 3d electrons localized in degeneracy states [22, 23]. The spin entropy contribution to the thermopower in the strong correlation system can be estimated by modified Heikes formula model [22, 23]:

$$S = -\frac{\kappa_B}{e} \ln \left[\frac{g_3}{g_4} \left(\frac{x}{1-x} \right) \right], \quad (1)$$

where g_3 and g_4 are the spin orbital degeneracy for Co^{3+} and Co^{4+} ions in the CoO_2 layer, respectively, x is Co^{4+} concentration in these layers, and κ_B is the Boltzmann constant. X-ray absorption and X-ray photoemission spectroscopy studies of $\text{Ca}_3\text{Co}_4\text{O}_{9+\delta}$ showed that CoO_2 layers have low-spin Co^{4+} and Co^{3+} configuration (t_{2g}^5 and t_{2g}^6) [8, 24]. The temperature dependence of the effective magnetic moment μ_{eff} is shown in Fig. 4. It is found that μ_{eff} for all doped samples with $x = 0.1, 0.2$, and 0.4 are

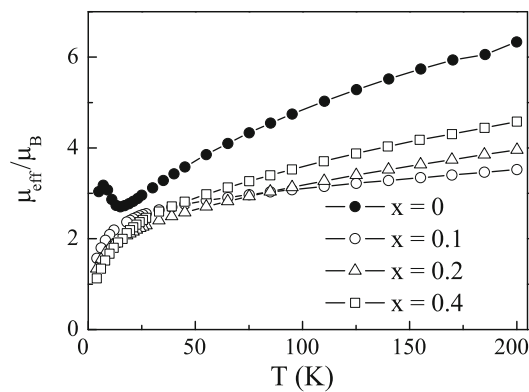


Fig. 4 Temperature dependence of the effective magnetic moment for $\text{Ca}_{3-x}\text{Lu}_x\text{Co}_4\text{O}_{9+\delta}$ ($x = 0, 0.1, 0.2$, and 0.4)

lower than that for $\text{Ca}_3\text{Co}_4\text{O}_{9+\delta}$ over the whole studied temperature range. The lower μ_{eff} in the doped samples is compatible with the low-spin configuration of the whole Co ions. This indicates that Lu substitution does not change the low-spin states of both Co^{4+} and Co^{3+} ions, consistent with the Refs. [25–27]. Therefore, it is plausible that the higher thermopower for Lu-doped samples may be ascribed to the decrease in Co^{4+} concentration. For Lu^{3+} is nonmagnetic ion, the reduction of μ_{eff} by Lu doping also provides evidence for the decrease in magnetic Co^{4+} ($S = 1/2$, $\mu_{\text{eff}} = 1.73 \mu_B$) concentration. Therefore, we conclude that the decrease in Co^{4+} concentration makes the thermopower increase. It is in agreement with the suggestion of Refs. [13, 28].

The measured resistivity as a function of temperature for $\text{Ca}_{3-x}\text{Lu}_x\text{Co}_4\text{O}_{9+\delta}$ materials is presented in Fig. 5. It is clear that the resistivity increases with increasing Lu doping level. The reason is that the substitution of trivalent Lu^{3+} for divalent Ca^{2+} decreases the concentration of holes. From Fig. 5, we can find that there is a transition from insulating to metallic behavior in samples with $x = 0, 0.1$, and 0.2 . The transition temperature $T_{\rho\min}$ is indicated by arrows, as seen in Fig. 5. The $\rho-T$ curve exhibits a metallic-like behavior above $T_{\rho\min}$ and a insulating behavior below $T_{\rho\min}$. $T_{\rho\min} = 86$ K for $x = 0$, 109 K for $x = 0.1$, and 188 K for $x = 0.2$. The transition temperature $T_{\rho\min}$ increases with increasing Lu doping level. For the sample with $x = 0.4$ showing insulating behavior in the whole studied temperature range, we speculate that $T_{\rho\min}$ is enhanced beyond the studied temperature regime.

The temperature dependence of the total thermal conductivity (κ) for $\text{Ca}_{3-x}\text{Lu}_x\text{Co}_4\text{O}_{9+\delta}$ ($x = 0, 0.1, 0.2$, and 0.4) samples is displayed in Fig. 6. κ of Lu-doped samples is far less than that of $\text{Ca}_3\text{Co}_4\text{O}_{9+\delta}$. Among this series, $\text{Ca}_{2.8}\text{Lu}_{0.2}\text{Co}_4\text{O}_{9+\delta}$ compound exhibits the lowest κ values. As we know, the total thermal conductivity consists of the electronic thermal conductivity (κ_e) and lattice thermal

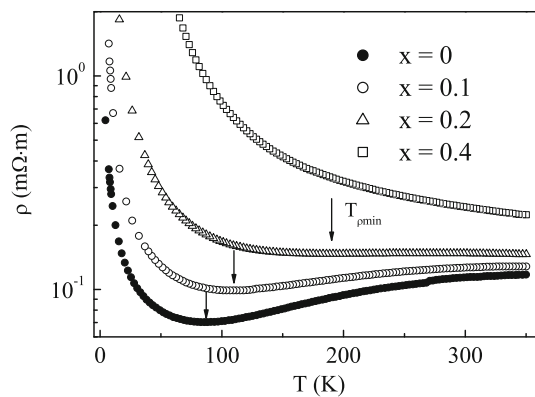


Fig. 5 Electrical resistivity as a function of temperature for $\text{Ca}_{3-x}\text{Lu}_x\text{Co}_4\text{O}_{9+\delta}$ ($x = 0, 0.1, 0.2$, and 0.4)

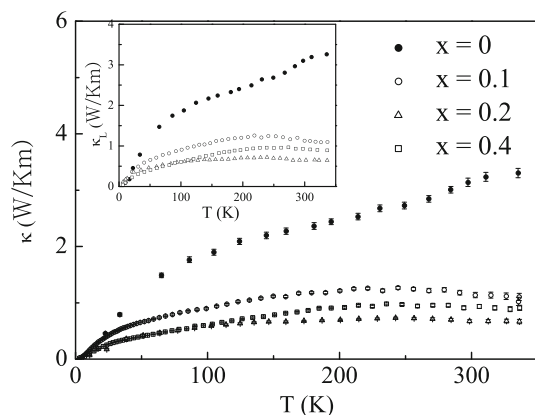


Fig. 6 Temperature dependence of the thermal conductivity for $\text{Ca}_{3-x}\text{Lu}_x\text{Co}_4\text{O}_{9+\delta}$ ($x = 0, 0.1, 0.2$, and 0.4). The *inset* shows the temperature dependence of the lattice thermal conductivity for these samples

conductivity (κ_L). The value of κ_e can be calculated using equation:

$$\kappa_e = L_0 T \sigma \quad (2)$$

where the Lorentz number (L_0) is equal to $2.44 \times 10^{-8} \text{ V}^2/\text{K}^2$, σ and T are the electrical conductivity and the absolute temperature, respectively. The lattice thermal conductivity (κ_L) has been calculated by subtracting κ_e from κ , which is shown in the inset of Fig. 6. It is found that the lattice thermal conductivity is the main source of the total thermal conductivity. Thus, the decrease in total thermal conductivity by Lu doping can mainly be attributed to the reduction of phonon contribution. Such reduction can be explained that the heavy element Lu dopant makes scattering phonons more effective and decreases the phonon thermal conductivity. This suggests that the lowest total thermal conductivity obtained for $\text{Ca}_{2.8}\text{Lu}_{0.2}\text{Co}_4\text{O}_{9+\delta}$ compound originates mainly from the decrease in lattice thermal conductivity.

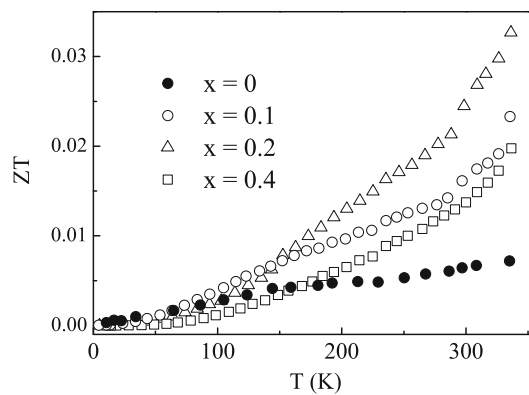


Fig. 7 Temperature dependence of ZT for $\text{Ca}_{3-x}\text{Lu}_x\text{Co}_4\text{O}_{9+\delta}$ ($x = 0, 0.1, 0.2$, and 0.4) ceramics

The thermoelectric figure of merit ZT as a function of temperature for $\text{Ca}_{3-x}\text{Lu}_x\text{Co}_4\text{O}_{9+\delta}$ series are calculated and shown in Fig. 7. Above 160 K, ZT values for doped samples are obviously enhanced and the $\text{Ca}_{2.8}\text{Lu}_{0.2}\text{Co}_4\text{O}_{9+\delta}$ material has the largest ZT values among these materials mainly due to its the lowest thermal conductivity. It can be seen that the figure of merit of this sample ($ZT = 0.032$) is about five times better than that of $\text{Ca}_3\text{Co}_4\text{O}_{9+\delta}$ ($ZT = 0.007$) at 335 K. Although $\text{Ca}_{2.6}\text{Lu}_{0.4}\text{Co}_4\text{O}_{9+\delta}$ sample has higher S than other samples, its ZT value remains quite low because of its high resistivity. In short, this study indicates that Lu doping can effectively enhance the thermoelectric performance of $\text{Ca}_3\text{Co}_4\text{O}_{9+\delta}$ -based thermoelectric materials.

Conclusion

The effects of Lu doping on thermoelectric properties of $\text{Ca}_3\text{Co}_4\text{O}_{9+\delta}$ have been systematically studied from 4 to 335 K. We find that the thermopower and resistivity for Lu-doped samples increase, while their thermal conductivity decreases. As a result, heavy Lu element doping induces much enhancement of thermoelectric figure of merit. Strikingly, for Lu-doped samples, the thermopower exhibits a steeper upturn at low temperatures.

Acknowledgements One of the authors (Prof. Z. H. Wang) would like to acknowledge financial support from the MOST 973 Program of China (No. 2008CB601003).

References

1. Snyder GJ, Toberer ES (2008) Nature 7:105
2. Terasaki I, Sasago Y, Uchinokura K (1997) Phys Rev B 56:R12685
3. Masset AC, Michel C, Maignan A, Hervieu M, Toulemonde O, Studer F, Raveau B, Hejtmanek J (2000) Phys Rev B 62:166

4. Wang Y, Rogado NS, Cava RJ, Ong NP (2003) *Nature* 423:425
5. Limelette P, Hébert S, Hardy V, Frésard R, Simon C, Maignan A (2006) *Phys Rev Lett* 97:046601
6. Taskin AA, Lavrov AN, Ando Y (2006) *Phys Rev B* 73:121101 (R)
7. Zhao BC, Sun YP, Lu WJ, Zhu XB, Song WH (2006) *Phys Rev B* 74:144417
8. Wakisaka Y, Hirata S, Mizokawa T, Suzuki Y, Miyazaki Y, Kajitani T (2008) *Phys Rev B* 78:235107
9. Shikano M, Funahashi R (2003) *Appl Phys Lett* 82:1851
10. Zhao BC, Sun YP, Song WH (2006) *J Appl Phys* 99:073906
11. Liu CJ, Huang LC, Wang JS (2006) *Appl Phys Lett* 89:204102
12. Zhang FP, Lu QM, Zhang JX (2009) *Physica B* 404:2142
13. Wang DL, Chen LD, Yao Q, Li JG (2004) *Solid State Commun* 129:615
14. Wang Y, Sui Y, Cheng JG, Wang XJ, Miao JP, Liu ZG, Qian ZN, Su WH (2008) *J Alloys Compd* 448:1
15. Pei J, Chen G, Lu DQ, Liu PS, Zhou N (2008) *Solid State Commun* 146:283
16. Lin YH, Lan JL, Shen ZJ, Liu YH, Nan CW, Li JF (2009) *Appl Phys Lett* 94:072107
17. Liu HQ, Zhao XB, Liu F, Song Y, Sun Q, Zhu TJ, Wang FP (2008) *J Mater Sci* 43:4933. doi:[10.1007/s10853-008-2990-6](https://doi.org/10.1007/s10853-008-2990-6)
18. Garde CS, Ray J (1995) *Phys Rev B* 51:2960
19. Sugiyama J, Itahara H, Tani T, Brewer JH, Ansaldi EJ (2002) *Phys Rev B* 66:134413
20. Tang GD, Wang ZH, Xu XN, Qiu L, Du YW (2010) *J Appl Phys* 107:053715
21. Terasaki I (2003) *Physica B* 328:63
22. Chaikin PM (1976) *Phys Rev B* 13:647
23. Koshiba W, Tsutsui K, Maekawa S (2000) *Phys Rev B* 62:6869
24. Mizokawa T, Tjeng LH, Lin HJ, Chen CT, Kitawaki R, Terasaki I, Lambert S, Michel C (2005) *Phys Rev B* 71:193107
25. Hebert S, Lambert S, Pelloquin D, Maignan A (2001) *Phys Rev B* 64:172101
26. Mizokawa T, Tjeng LH, Steeneken PG, Brookes NB, Tsukada I, Yamamoto T, Uchinokura K (2001) *Phys Rev B* 64:115104
27. Zhang FP, Lu QM, Zhang JX, Zhang X (2009) *J Alloys compd* 477:543
28. Asahi R, Sugiyama J, Tani T (2002) *Phys Rev B* 66:155103